**TITLE: Locating ligand binding sites in G-protein coupled receptors using combined information from docking and sequence conservation**

Authors: Ashley R. Vidad*[1], Stephen Macaspac*[1] & Ho-Leung Ng[1,2,3#]

[1]University of Hawaii at Manoa, Department of Chemistry, Honolulu, HI. USA
[2]University of Hawaii Cancer Center, Honolulu, HI. USA
[3]Kansas State University, Department of Biochemistry & Molecular Biophysics, Manhattan, KS. USA

* Authors are considered equal contributors to this paper.
[#] Corresponding author. hng@ksu.edu

**Abstract**

G-protein coupled receptors (GPCRs) are the largest protein family of drug targets. Detailed mechanisms of binding are unknown for many important GPCR-ligand pairs due to the difficulties of GPCR expression, biochemistry, and crystallography. We describe our new method, ConDock, for predicting ligand binding sites in GPCRs using combined information from surface conservation and docking starting from crystal structures or homology models. We demonstrate the effectiveness of ConDock on well-characterized GPCRs such as the β2 adrenergic and A2A adenosine receptors. We also use ConDock to predict ligand binding sites on GPER, the G-protein coupled estrogen receptor, for four ligands: estradiol, G1, G15, and tamoxifen. ConDock predicts that all four ligands bind to the same location on GPER, centered on L119, H307, and N310; this site is deeper in the receptor cleft than predicted by previous studies. We compare the sites predicted by ConDock and traditional methods that utilize information from surface geometry, surface conservation, and ligand chemical interactions. Incorporating sequence conservation information in ConDock overcomes errors introduced from physics-based scoring functions and homology modeling.

## Introduction

GPCRs (G-protein coupled receptors) are the largest family of drug targets and the targets of >30% of all drugs. Because they are membrane proteins with flexible and dynamic structures, biochemical and crystallography experiments are difficult. Only ~50 GPCRs out of > 800 in the human genome have been crystallized despite their great pharmacological importance. Recent advances in homology modeling have allowed more accurate ligand docking (1), but GPCR modeling remains challenging due to structural flexibility and abundance of flexible loops.

Various computational approaches have been used to predict ligand binding sites in G-protein coupled receptors. Traditional docking methods compute the lowest energy pose of a ligand fit to a receptor surface. Such methods are highly dependent on the form of the energy scoring function and accuracy of the receptor model structure (2–4). These methods have been used to identify ligand binding sites and build pharmacophores for G-protein coupled receptors (GPCRs) (5–7), but the lack of diverse GPCR crystal structures presents serious challenges to using docking methods for identification of ligand binding sites. An underappreciated feature that can be used to predict ligand binding sites is surface or sequence conservation. Binding sites for particular ligands are often conserved, although systematic sequence variation can encode ligand specificity (8–10). The massive abundance of genomic data for GPCRs can provide strong constraints for possible ligand binding sites even without chemical or structural information (11–13).

There has been less research on methods that combine information from chemical interactions, geometric surface analysis, and bioinformatics. Hybrid strategies, such as Concavity (14), have demonstrated superior performance in predicting ligand binding sites compared to

single-mode approaches. Concavity scores binding sites by evolutionary sequence conservation as quantified by the Jensen-Shannon divergence (10) and employs geometric criteria of size and shape. Here, we describe and apply a new hybrid strategy, ConDock, that combines information from surface conservation with intermolecular interactions from docking calculations. We compare our results from those previously published using purely docking-based and other hybrid methods (15, 16). We demonstrate the effectiveness of ConDock for identifying ligand binding sites for two GPCRs with known crystal structures, the β2 adrenergic and A2A adenosine receptors.

We also apply ConDock to predict the binding sites of four ligands to the less characterized G-protein coupled estrogen receptor (GPER, formerly known as GPR30), a membrane-bound estrogen receptor. GPER is proposed to mediate rapid estrogen-associated effects, cAMP regeneration, and nerve growth factor expression (17–21). GPER is known to bind estradiol and the estrogen receptor inhibitor breast cancer drugs, tamoxifen and fulvestrant (Fig. S1). Recently, GPER-specific ligands G1 and G15 were discovered (22, 23). G1 and G15 are structurally similar, differing by only an acetyl group. G1 is an agonist, whereas G15 is an antagonist. No crystal structure of GPER is available, and details of ligand binding are unknown. We discuss how the ConDock-predicted binding sites provide a basis for G1 and G15 binding specificity.

## Results

The A2A adenosine and β2 adrenergic receptors are the most heavily studied GPCRs with crystal structures available. We used them as standards to validate the effectiveness of ConDock for predicting ligand binding sites. For both receptors, we ranked the ligand binding

sites predicted by the docking program, SwissDock, with the ConDock scoring function (Table 1). Residues within 3.5 Å of the highest scoring predicted ligand sites were compared with the poses in the crystal structures. In addition, we determined the distance between the center of mass for the crystal structure ligand binding locations and the predicted binding site locations.

**Table 1. Comparison of ConDock predicted and crystal structure ligand binding sites**

| GPCR | Ligand | Distance to crystal structure pose (Å) | Consurf conservation score | SwissDock energy Score | Combined ConDock score |
|---|---|---|---|---|---|
| A2A adenosine receptor | adenosine (agonist) | 1.8 | 0.86 | -1702.1 | -1458.9 |
| A2A adenosine receptor | ZM241385 (inverse agonist) | 1.0 | 0.86 | -1534.6978 | -1319.8 |
| β2 adrenergic receptor | epinephrine (agonist) | 0.4 | 0.87 | -1119.98 | -970.7 |
| β2 adrenergic receptor | carazolol (inverse agonist) | 1.8 | 0.78 | -1534.6978 | -1319.8 |

The highest ranked pose for adenosine within the A2A adenosine receptor was within 1.8 Å of the ligand position in the crystal structure. The top predicted binding site for adenosine was within a pocket bound by A63, A81, F168, E169, N253, I274, and H278 (Fig. 1). This pose possessed the highest conservation score among all predicted binding sites at 0.86. In this pose there is a hydrogen bond between the ethoxy group on the ribose ring of adenosine and the

carboxyl terminal of A81, between the amino group of the benzyl ring and the terminal carboxy group of the E169, and between a hydroxyl group of adenosine and the secondary amine of H78. Hydrophobic interactions are present between adenosine and nonpolar residues A63, F168, I274.

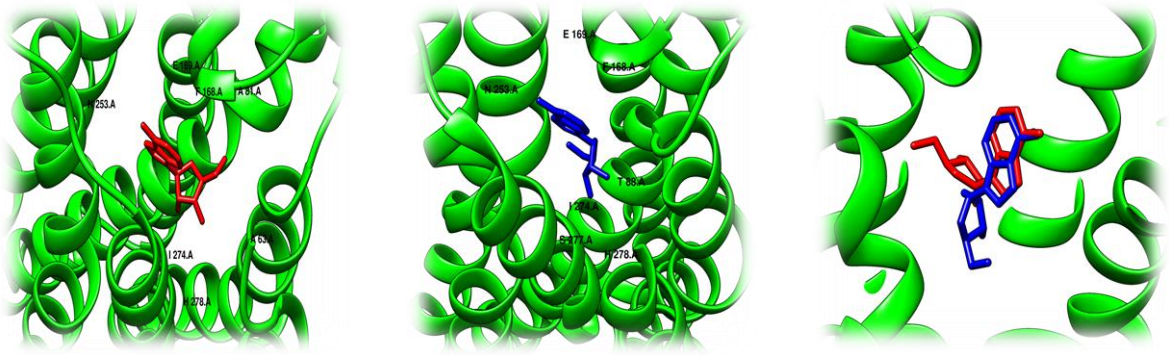

A B C

**Figure 1. Predicted adenosine binding sites in A2A adenosine receptor.** A) Highest scoring docking pose for adenosine B) Crystal structure adenosine orientation C) Crystal structure ligand orientation and highest scoring pose superimposed.

The highest ranked site for ZM241385 within the A2A adenosine receptor was within 1.0 Å of the ligand's position in the crystal structure. In this top pose, ZM241385 is found within the pocket bound by S67, F168, E169, N253, and I274 (Fig. 2). This orientation yielded a conservation score of 0.86. There is hydrogen bonding between the secondary amine substituent of ZM241385 with the terminal amide of N253 and the carboxyl group of E169. Hydrophobic interactions are observed between ZM241385 and non-polar residues F168 and I274.

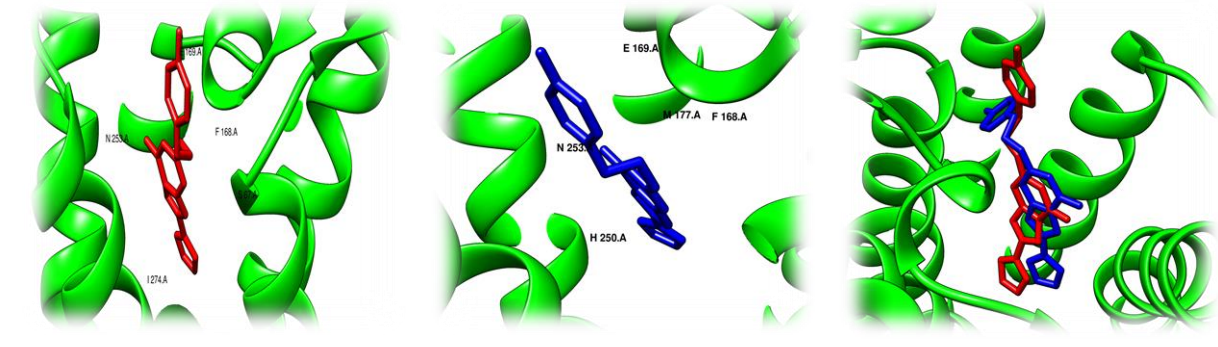


A B C

**Figure 2. Predicted ZM241385 binding sites in A2A adenosine receptor.** A) Highest scoring docking pose for ZM241385 B) Crystal structure showing adenosine orientation C) Crystal structure ligand orientation and highest scoring pose superimposed.

The highest ranked pose for epinephrine within the β2 adrenergic receptor was within 0.4 Å of the ligand position within the crystal structure (4LDO). This binding site for epinephrine was within the pocket bound by D113, N293, and N312 (Fig. 3). Hydrogen bonding is present between the secondary hydroxyl group of epinephrine and the terminal carboxyl group of D113 and the secondary amine of epinephrine and the terminal carboxyl group of D113. No hydrophobic interactions are observed between epinephrine and the β2 adrenergic receptor.

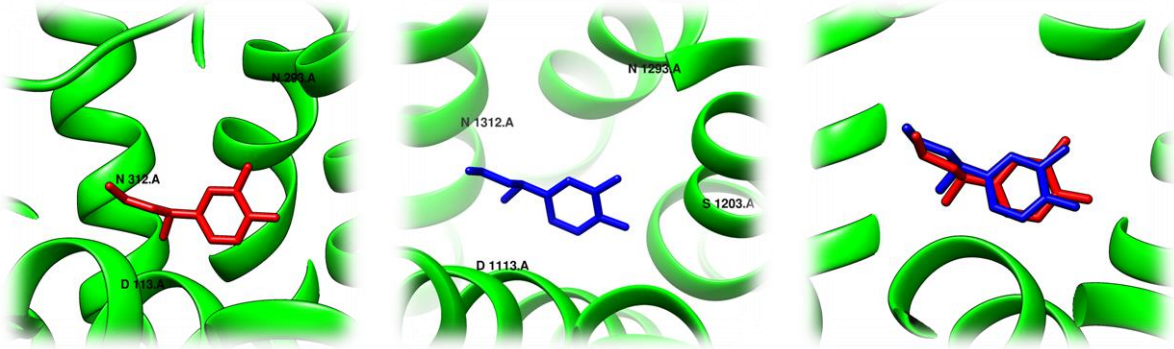


A B C

**Figure 3. Predicted epinephrine binding sites in β2 adrenergic receptor.** A) Highest scoring docking pose for epinephrine. B) Crystal structure showing epinephrine orientation. C) Crystal structure ligand orientation and highest scoring pose superimposed.

The highest ranked pose for carazolol within the β2 adrenergic receptor was within 1.8 Å of the ligands position within the crystal structure (2RH1). This binding site for carazolol was within the pocket bound by D113, F193, N293, Y308, and N312 (Fig. 4). This pose possessed the highest conservation score among all predicted binding sites at 0.86. Hydrogen bonding is present between the secondary amine of carazolol with the hydroxyl group of N312 and between the hydroxyl group of carazolol with the hydroxyl group of D113. Hydrophobic interactions are observed between the carazalol and F193.

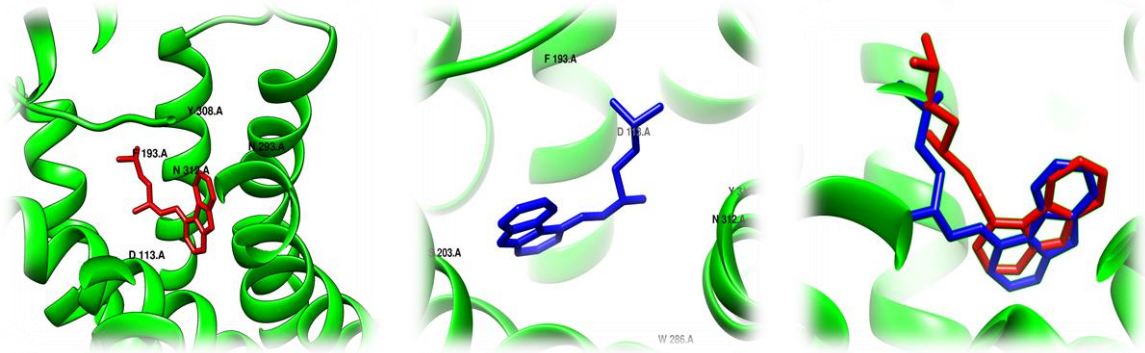


A B C

**Figure 4. Predicted carazolol binding sites in β2 adrenergic receptor.** A) Highest scoring docking pose for carazolol. B) Crystal structure showing carazolol orientation. C) Crystal structure ligand orientation and highest scoring pose superimposed.

To predict potential ligand binding sites in GPER, we first created a homology model using GPCR-I-TASSER (24), that has been shown to be the most accurate GPCR homology

modeling software package. GPCR-I-TASSER identified the closest matching crystal structure to GPER to be the CCR5 chemokine receptor (PDB 4mbs) with 23% sequence identity. GPCR-I-TASSER used this crystal structure along with 9 other GPCR crystal structures as templates for homology modeling. The GPER homology model differs from chain A of the crystal structure of CCR5 chemokine receptor with RMSD of 0.96 Å across Cα atoms (Fig. S2). The primary differences are in the extracellular loop between helices 4 and 5 and the intracellular loops between helices 5 and 6, and after helix 7. These two intracellular loops are predicted by ERRAT (25) to be the least reliable based on the likelihood of atom pair type interactions from high resolution crystal structures. As the sites with the greatest predicted errors are on the intracellular face of GPER, far from the ligand binding site, they are less likely to affect our ligand prediction study, giving us greater confidence in our homology model. It should be noted that ERRAT was not developed for analyzing membrane proteins so the reliability of its error analysis for the GPER homology model is uncertain.

Using the SwissDock server (26), we docked structures of the four ligands E2, G1, G15, and tamoxifen (Fig. S1) to the homology model of GPER. Most of the docked sites from SwissDock were not located on the extracellular face of GPER and thus were considered nonviable (Fig. S3). The shortcomings of a purely physics based scoring function such as that used by SwissDock in predicting ligand binding is not surprising given the lack of an experimental crystal structure and well known limitations of current computational methodology (27–30).

We next ranked all ligand binding sites generated by SwissDock that were located on the extracellular face of GPER using the combined ConDock score. The ConDock score is simply the product of the ConSurf (31, 32) binding surface sequence conservation score and the

SwissDock FullFitness energy score (33). A highly negative ConDock score is associated with a more probable ligand binding site. For all four ligands, the ConDock score identified one or two ligand binding sites and poses that clearly outscored other candidates (Table 2). ConDock identified the same approximate binding site for all four ligands, although this was not an explicit criterion in the calculations (Fig. 5). The average ConSurf conservation score across the four ligand binding sites is 0.82, indicating that the site is highly but not completely conserved. The binding site is located deep in the receptor cleft, although this too was not a criterion in the prediction calculation. Given the lack of additional experimental evidence for the location of the ligand binding site, the proposed ConDock sites are physically reasonable.

| Ligand | ConSurf conservation score | SwissDock energy score | Combined ConDock score |
|---|---|---|---|
| E2, pose 1 | 0.84 | -964.9 | -813.2 |
| E2, pose 2 | 0.80 | -967.9 | -774.3 |
| G1 | 0.85 | -970.7 | -825.1 |
| G15 | 0.8 | -974.6 | -779.7 |
| Tamoxifen, pose 1 | 0.81 | -947.9 | -763.6 |
| Tamoxifen, pose 2 | 0.81 | -947.5 | -763.6 |

**Table 2. Scores for predicted binding sites and poses for GPER ligands.**

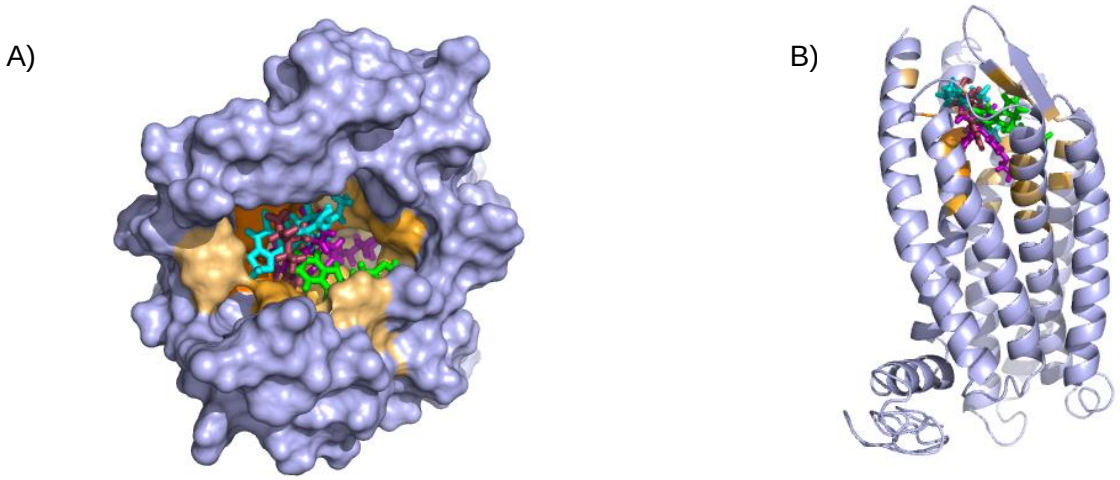


**Figure 5. Predicted ligand binding pockets in GPER.** A) Extracellular perspective of GPER showing amino acids predicted to contact ligands E2 (maroon), G1 (cyan), G15 (green), and tamoxifen (violet). Residues colored orange are predicted to contact one or more ligands with darker hue indicating interaction with multiple ligands. B) Predicted binding pocket viewed from a 90° rotation.

We found two promising binding sites for E2 in GPER. The two sites are 4.4 Å apart, located deep in the receptor cleft (Fig. 6). E2 is oriented perpendicular to the lipid membrane and rotated about 180° between the two poses. The conservation scores for these two poses are 0.84 and 0.80. The energy scores of the two poses are similar. The amino acids contacting E2 in pose 1 are conserved in GPERs from six species, and only one residue contacting pose 2, H282, varies across species. In the top ranked pose, there is a hydrogen bond between the inward pointing D-ring hydroxyl group of E2 and the carboxyl terminal on E115. Hydrophobic interactions are present between E2 and non-polar residues L119, Y123, P303, and F314. In the second ranked pose, the inward pointing A-ring hydroxyl group of E2 makes a hydrogen bond with N310. This pose is in a less hydrophobic environment, contacting primarily H282 and P303.

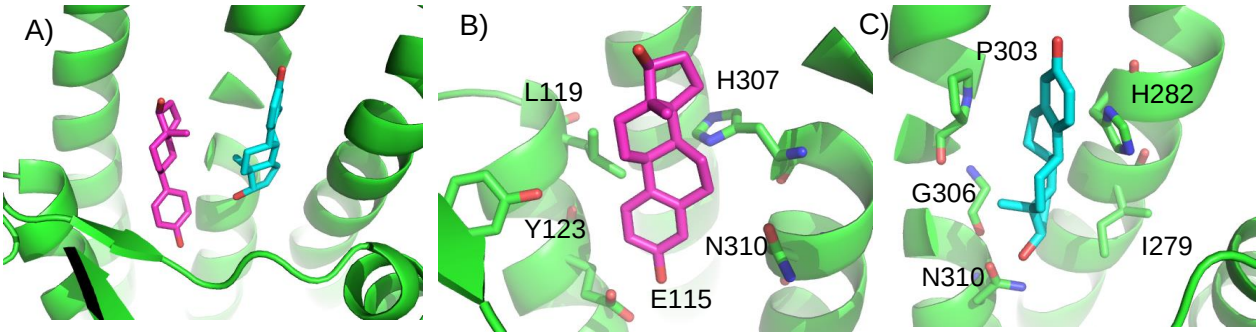


**Figure 6. Predicted E2 binding sites in GPER.** A) The two highest scoring docking poses for E2. B) Receptor-ligand interactions for E2 pose 1. C) Receptor-ligand interactions for E2 pose 2.

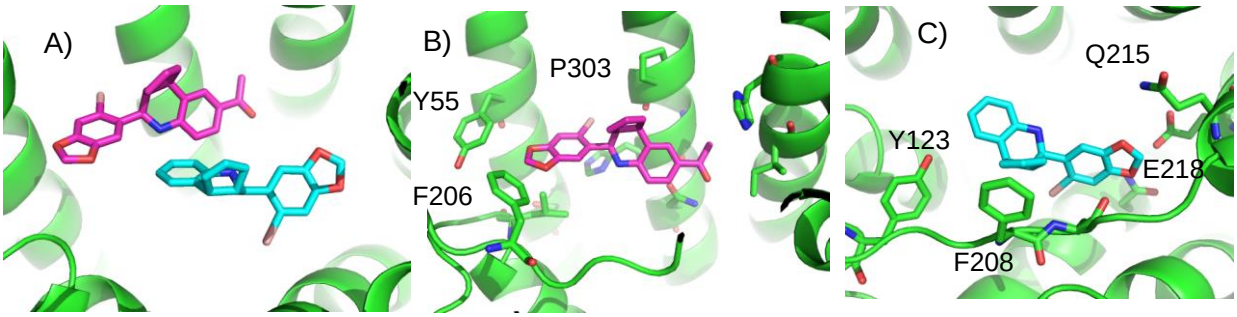


**Figure 7. Predicted G1 and G15 binding sites in GPER.** A) The highest scoring docking poses for G1 (maroon) and G15 (cyan). B) Receptor-ligand interactions for G1. C) Receptor-ligand interactions for G15.

ConDock predicts that G1 and G15 bind in adjacent but distinct binding sites separated by 2.3 Å despite the chemical similarity of the two ligands. The top predicted binding site for G1 is found within the pocket bound by Y55, L119, F206, Q215, I279, P303, H307, and N310 (Fig. 7). This orientation had the highest conservation score of all predicted binding sites at 0.85. In this pose, N310 makes a long hydrogen bond with the acetyl oxygen of G1. The predicted binding site for G15 is found within the pocket bound by L119, Y123, M133, S134, L137, Q138, P192, V196, F206, C207, F208, A209, V214, E218, H307, and N310. This pose had a conservation score of

0.8. Hydrogen bonding is not observed between GPER and G15. Hydrophobic interactions are observed with L119, Y123, F206, and V214. An interesting aspect of this binding site is that the amino acid at position 214 is valine in humans but is isoleucine in Atlantic croaker and zebrafish. These two hydrophobic amino acids differ by only a methyl group.

ConDock predicted two equally high scoring, overlapping poses for tamoxifen, near E115, L119, Y123, L137, Q138, M141, Y142, Q215, E218, W272, E275, I279, P303, G306, H307, and N310 (Fig. 8). The conservation score of this orientation is 0.81. Hydrophobic interactions are observed between tamoxifen and non-polar residues L119, Y123, Y142, P303, and F314. Notably, the amine group of tamoxifen is neutralized by E218 and E275.

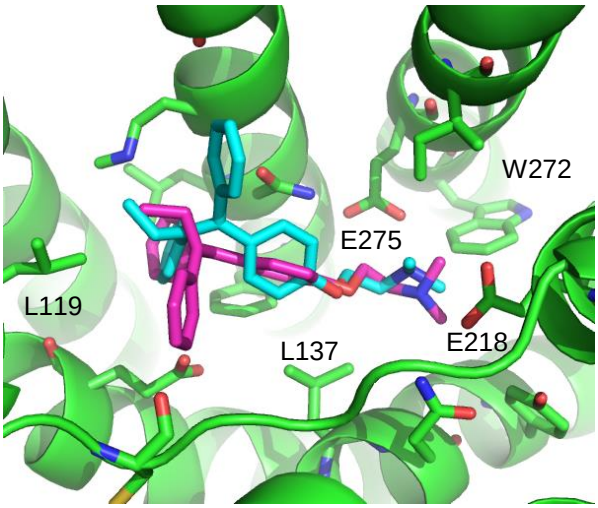


**Figure 8. Predicted tamoxifen binding sites in GPER.** A) The highest scoring docking poses for tamoxifen, pose 1 (maroon) and pose 2 (cyan).

In comparison with the ligand binding sites predicted by traditional methods based on surface geometry and conservation, the site predicted by ConDock is more detailed and of higher resolution due to the information from chemical interactions from ligand docking. Moreover,

prediction methods based on surface geometry and conservation cannot differentiate between binding sites for different ligands. We compared the ligand binding site predicted by ConDock to those predicted by three other software packages representing different approaches: CASTp (34), which analyzes surface geometry, SiteHound (35), which maps surfaces with a chemical probe, and Concavity (14), which analyzes surface geometry and conservation (Fig. 9). All three methods could identify a ligand binding site roughly matching that from ConDock. The pocket predicted by ConDock is deeper than the other pockets, which while intuitively attractive is not necessarily correct. SiteHound performed particularly poorly, with the top scoring site located on the GPER intracellular face. The site identified by SiteHound closest to the ConDock site was scored third and is a shallow binding pocket near H52-G58, E275-H282, and R299-H307 (Fig. 9C). In contrast, the Concavity site was smaller and shallower than the ConDock site (Fig. 9D). Surprisingly, the site predicted by the simpler CASTp method best matched the ConDock site but is also smaller and shallower (Fig. 9B). For proteins such as GPCRs with large, concave binding pockets, geometry-based prediction methods such as Concavity and CASTp can easily identify the general location of the binding site. However, such methods may have more difficulty recovering the specific, ligand-specific binding site. It is also surprising that ConDock more closely matched the results of the geometry-based methods given that ConDock does not take surface geometry into account. Without experimental data, it is not possible to conclude which of the predicted binding sites is correct at this time.

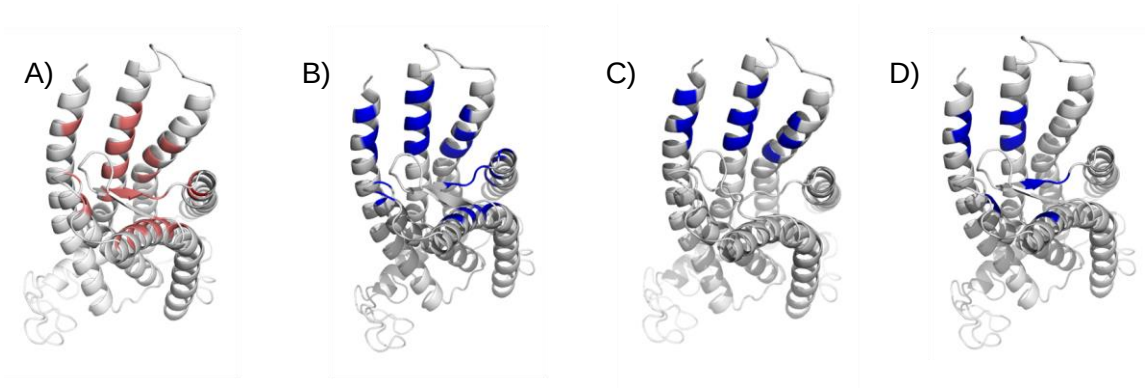


**Figure 9. Predicted ligand binding sites by ConDock, CASTp, SiteHound, Concavity.** Ligand binding sites are colored, predicted by A) ConDock, B) CASTp, C) SiteHound, D) Concavity.

## Discussion

The ConDock scoring method, incorporating information from both surface conservation and docking binding energy, was used to predict viable ligand binding sites for four different GPER ligands. In contrast to more typical geometry-based ligand binding site prediction methods, ConDock scoring takes advantage of chemistry-specific information about the ligand-receptor interface. The poor performance of SiteHound in predicting ligand binding sites on GPER suggests that a method based only on chemical interactions or docking is highly susceptible to error, most likely due to the inadequate accuracy of homology models. Surface conservation data not only provides orthogonal knowledge but also dampens the influence from the shortcomings of current computational methods in homology modeling, docking, and predicting binding affinity. How best to mathematically combine these multiple data sources has been debated (10, 14), but we demonstrate here that a simple product function is effective. Although the ligands analyzed differ greatly in chemical structure, the ConDock scoring method predicted that all four bind to the same approximate region, deep in the extracellular cleft of the

receptor. Undoubtedly, further refinement of a hybrid scoring function will lead to improved predictions.

Recent GPER modeling studies using molecular dynamics simulations and docking identified different potential binding sites for E2, G1, and G15 near F206 and F208; the interaction with this region was described as driven primarily by π-π stacking interactions (15, 16). Figure 10 compares the ConDock binding site against that predicted in the molecular dynamics simulation and docking study. The ConDock binding site is located deeper in the extracellular cleft; the other proposed site mostly involved surface exposed loops. Mendez-Luna *et al*. proposed that Q53, Q54, G58, C205, and H282 all interact with G1 and G15; however, none of these residues are conserved across the six species we analyzed. Experimental data is not currently available to support one model over the other.

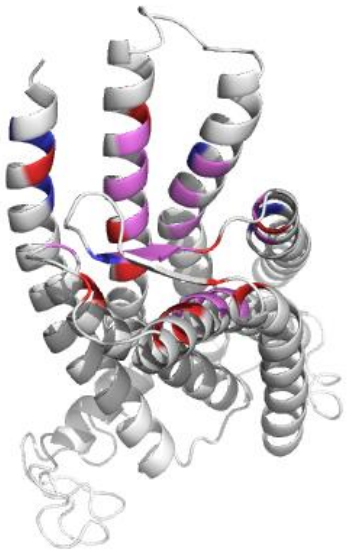

**Figure 10. Comparison of proposed ligand binding sites.** Comparison of the ConDock ligand binding site (red) with that proposed by Mendez-Luna *et al.* (blue). Residues found in both sites are colored violet.

In summary, the simple ConDock hybrid scoring model predicts physically plausible ligand binding sites by combining information from ligand docking and surface conservation. Using multiple orthogonal sources of information avoids errors introduced by modeling, especially in a case where a crystal structure of the receptor is unavailable. Using this hybrid method, we identified a site in the extracellular cleft of GPER that has the potential to bind four known GPER ligands. Further optimization of hybrid scoring functions should yield significantly improved predictions.

## Methods

### Protein conservation

GPCR protein sequences were acquired from Uniprot database (36). Only Swiss-Prot (37) curated sequences were compared using the Align function of UniProt. For the A2A adenosine receptor, the protein sequences aligned were from *Homo sapiens*, *Canis familiaris*, *Xenopus tropicalis*, *Myotis davidii*, *Loxodonta africana*, *Gallus gallus*, *Anolis caronlinesis*, *Oncorhynchus mykiss*, *Ailuropoda melanoleuca*, and *Alligator mississippiensis*. For the β2 adrenergic receptor, the protein sequences aligned were from *Homo sapiens*, *Oncorhynchus mykiss*, *Myotis brandtii*, *Callorhinchus milii*, *Ophiophagus hannah*, *Canis familiaris*, *Loxodonta africana*, *Ailuropoda melanoleuca*, *Ficedula albicollis*, and *Xenopus laevis*. GPER protein sequences aligned were from diverse species: *Homo sapiens*, *Rattus norvegicus*, *Mus musculus*, *Macaca mulatta*, *Danio rerio*, and *Micropogonias undulatus*. The multiple sequence alignment file was submitted to ConSurf (31, 32). ConSurf assesses conservation using Bayesian reconstruction of a phylogenetic tree. Each sequence position is scored from 0-9, where 9 indicates that the amino acid was retained in all the organisms (Fig. S4). Values from ConSurf were mapped onto the receptor surface with Chimera (38).

**Homology modeling and docking**

The crystal structures for the A2A adenosine receptor and the β2 adrenergic receptor were acquired from the RCSB protein data bank: β2 adrenergic receptor bound to epinephrine (PDB 4ldo), β2 adrenergic receptor bound to carazolol (PDB 2rh1), A2A adenosine receptor bound to adenosine (PDB 2ydo), and A2A adenosine receptor bound to ZM241385 (PDB 5k2a). These structures were prepped for docking with Chimera by removing extraneous chains and

bound ligands. Coordinates for epinephrine, carazolol, adenosine, and ZM241385 were obtained from the ZINC database (39). Ligands were docked into receptors with SwissDock (26).

The crystal structure of GPER has not yet been determined. We created a homology model using GPCR I-TASSER (Iterative Threading Assembly Refinement), the most accurate homology modeling software customized for GPCRs (24). GPCR I-TASSER modeled the GPER structure using templates from the ten closest related GPCR crystal structures (PDB 4mbs, 2ks9, 1kpn, 1u19, 2ziy, 1kp1, 3odu, 4ea3, 4iaq, 2y00). The homology model was validated with ERRAT (25). Coordinates for E2, G1, G15, and tamoxifen were downloaded from the ZINC ligand database (39) and submitted to SwissDock (26) for docking. SwissDock is a web interface to the EADock DSS (33) engine, which performs blind, global (does not require targeting of a particular surface) docking using the physics based CHARMM22 force field (40). The "FullFitness Score" calculated by SwissDock using clustering and the FACTS implicit solvent model (41) was used as the "Energy Score" for our calculations.

**Combined analysis**

SwissDock poses were manually screened for those binding sites located on or near the extracellular side of the protein. Ligand binding surfaces included residues within 3.5 Å from the docked ligand. The average conservation score of the amino acids that were highlighted served as the "Conservation Score" of that specific orientation (Fig. 11). The combined ConDock score is defined as the product of the Conservation and Energy Scores. As the Energy Score is a modified free energy function, a highly negative ConDock score is associated with a more probable ligand binding site. Binding sites predicted by ConDock results were compared with those predicted by CASTp (34), SiteHound (35), and Concavity (14). For CASTp, SiteHound,

and Concavity, ligand binding pockets were defined as residues within 4 Å of the selected probe/cluster.

$$\textbf{Combined ConDock Score} = (\text{Conservation Score}) * (\text{Energy Score})$$

$$\textbf{Conservation Score} = \frac{1}{10}\frac{\sum_{k=1}^{n}(\text{Amino Acid ConSurf Score})_k}{n}$$

$$\textbf{Energy Score} = \text{SwissDock FullFitness Score}$$

**Figure 11. Calculation of combined ConDock scores for ligand binding sites.** The Conservation Score is calculated over the *n* residues in a binding site, indexed by *k*.

**Crystal structure benchmarks**

The coordinates for the crystal structures of the A2A adenosine receptor (2ydo and 5k2a) and β2 adrenergic receptor (2rh1 and 4ldo) were uploaded to Chimera. Each receptor was screened for residues within 3.5 Å of their respective ligands. These residues served as a benchmark of comparison for the predicted sites contrived by the ConDock scoring function. For the A2A adenosine receptor, adenosine is found within the pocket bound by T88, Fl68, E169, N253, I274, S277, and H278. ZM241385 is found within the pocket bound by F168, E169, M177, H250, and N253. In the β2 adrenergic receptor, epinephrine is found within the pocket bound by D113, S203, N293, N312. Carazolol is found within the pocket bound by D113, F193, S203, W286, N312, Y316.

**Acknowledgements**

This work was funded by the Victoria S. and Bradley L. Geist Foundation (H.L.N.), NSF CAREER Award 1350555 (H.L.N.), and the Undergraduate Research Opportunities Program at the University of Hawaii at Manoa (A.R.V., S.M.).

**Author contributions**

A.R.V., S.M., and H.L.N. performed the analysis and calculations. A.R.V., S.M., and H.L.N. wrote the manuscript. H.L.N. supervised the project.

**Competing financial interests**

The authors have no competing financial interests.

## References


1. Feng X, Ambia J, Chen K-YM, Young M, Barth P (2017) Computational design of ligand-binding membrane receptors with high selectivity. *Nat Chem Biol* 13(7):715–723.

2. Shoichet BK, Kobilka BK (2012) Structure-based drug screening for G-protein-coupled receptors. *Trends Pharmacol Sci* 33(5):268–272.

3. Katritch V, Abagyan R (2011) GPCR agonist binding revealed by modeling and crystallography. *Trends Pharmacol Sci* 32(11):637–643.

4. Katritch V, Rueda M, Lam PC-H, Yeager M, Abagyan R (2010) GPCR 3D homology models for ligand screening: lessons learned from blind predictions of adenosine A2a receptor complex. *Proteins* 78(1):197–211.

5. Sanders MPA, et al. (2011) Snooker: A Structure-Based Pharmacophore Generation Tool Applied to Class A GPCRs. *J Chem Inf Model* 51(9):2277–2292.

6. Kratochwil NA, et al. (2011) G protein-coupled receptor transmembrane binding pockets and their applications in GPCR research and drug discovery: a survey. *Curr Top Med Chem* 11(15):1902–1924.

7. Tang H, Wang XS, Hsieh J-H, Tropsha A (2012) Do crystal structures obviate the need for theoretical models of GPCRs for structure-based virtual screening? *Proteins* 80(6):1503–1521.

8. Wass MN, Sternberg MJE (2009) Prediction of ligand binding sites using homologous structures and conservation at CASP8. *Proteins Struct Funct Bioinforma* 77(S9):147–151.

9. Kalinina OV, Gelfand MS, Russell RB (2009) Combining specificity determining and conserved residues improves functional site prediction. *BMC Bioinformatics* 10:174.

10. Capra JA, Singh M (2007) Predicting functionally important residues from sequence conservation. *Bioinformatics* 23(15):1875–1882.

11. Madabushi S, et al. (2004) Evolutionary Trace of G Protein-coupled Receptors Reveals Clusters of Residues That Determine Global and Class-specific Functions. *J Biol Chem* 279(9):8126–8132.

12. Levit A, Barak D, Behrens M, Meyerhof W, Niv MY (2012) Homology model-assisted elucidation of binding sites in GPCRs. *Methods Mol Biol Clifton NJ* 914:179–205.

13. Sanders (2011) ss-TEA: Entropy based identification of receptor specific ligand binding residues from a multiple sequence alignment of class A GPCRs. *BMC Bioinformatics* 12(Suppl 6):332–343.

14. Capra JA, Laskowski RA, Thornton JM, Singh M, Funkhouser TA (2009) Predicting Protein Ligand Binding Sites by Combining Evolutionary Sequence Conservation and 3D Structure. *PLoS Comput Biol* 5(12):e1000585.

15. Méndez-Luna D, et al. (2015) Deciphering the GPER/GPR30-agonist and antagonists interactions using molecular modeling studies, molecular dynamics, and docking simulations. *J Biomol Struct Dyn* 33(10):2161–2172.

16. Arnatt CK, Zhang Y (2013) G Protein-Coupled Estrogen Receptor (GPER) Agonist Dual Binding Mode Analyses Toward Understanding of Its Activation Mechanism: A Comparative Homology Modeling Approach. *Mol Inform* 32(7):647–658.

17. Carmeci C, Thompson DA, Ring HZ, Francke U, Weigel RJ (1997) Identification of a Gene (GPR30) with Homology to the G-Protein-Coupled Receptor Superfamily Associated with Estrogen Receptor Expression in Breast Cancer. *Genomics* 45(3):607–617.

18. Kvingedal AM, Smeland EB (1997) A novel putative G-protein-coupled receptor expressed in lung, heart and lymphoid tissue. *FEBS Lett* 407(1):59–62.

19. O'Dowd BF, et al. (1998) Discovery of Three Novel G-Protein-Coupled Receptor Genes. *Genomics* 47(2):310–313.

20. Filardo EJ, Quinn JA, Frackelton AR, Bland KI (2002) Estrogen Action Via the G Protein-Coupled Receptor, GPR30: Stimulation of Adenylyl Cyclase and cAMP-Mediated Attenuation of the Epidermal Growth Factor Receptor-to-MAPK Signaling Axis. *Mol Endocrinol* 16(1):70–84.

21. Kanda N, Watanabe S (2003) 17β-Estradiol Enhances the Production of Nerve Growth Factor in THP-1-Derived Macrophages or Peripheral Blood Monocyte-Derived Macrophages. *J Invest Dermatol* 121(4):771–780.

22. Bologa CG, et al. (2006) Virtual and biomolecular screening converge on a selective agonist for GPR30. *Nat Chem Biol* 2(4):207–212.

23. Dennis MK, et al. (2009) In vivo Effects of a GPR30 Antagonist. *Nat Chem Biol* 5(6):421–427.

24. Zhang J, Yang J, Jang R, Zhang Y (2015) GPCR-I-TASSER: A Hybrid Approach to G Protein-Coupled Receptor Structure Modeling and the Application to the Human Genome. *Structure* 23(8):1538–1549.

25. Colovos C, Yeates TO (1993) Verification of protein structures: patterns of nonbonded atomic interactions. *Protein Sci Publ Protein Soc* 2(9):1511–1519.

26. Grosdidier A, Zoete V, Michielin O (2011) SwissDock, a protein-small molecule docking web service based on EADock DSS. *Nucleic Acids Res* 39(suppl):W270–W277.

27. Merz KM (2010) Limits of Free Energy Computation for Protein−Ligand Interactions. *J Chem Theory Comput* 6(5):1769–1776.

28. Wan S, Knapp B, Wright DW, Deane CM, Coveney PV (2015) Rapid, Precise, and Reproducible Prediction of Peptide–MHC Binding Affinities from Molecular Dynamics That Correlate Well with Experiment. *J Chem Theory Comput* 11(7):3346–3356.

29. Li Y, Hou T, Goddard III W (2010) Computational Modeling of Structure-Function of G Protein-Coupled Receptors with Applications for Drug Design. *Curr Med Chem* 17(12):1167–1180.

30. Smith RD, et al. (2015) CSAR Benchmark Exercise 2013: Evaluation of Results from a Combined Computational Protein Design, Docking, and Scoring/Ranking Challenge. *J Chem Inf Model*. doi:10.1021/acs.jcim.5b00387.

31. Armon A, Graur D, Ben-Tal N (2001) ConSurf: an algorithmic tool for the identification of functional regions in proteins by surface mapping of phylogenetic information1. *J Mol Biol* 307(1):447–463.

32. Ashkenazy H, Erez E, Martz E, Pupko T, Ben-Tal N (2010) ConSurf 2010: calculating evolutionary conservation in sequence and structure of proteins and nucleic acids. *Nucleic Acids Res* 38(Web Server issue):W529-533.

33. Grosdidier A, Zoete V, Michielin O (2011) Fast docking using the CHARMM force field with EADock DSS. *J Comput Chem* 32(10):2149–2159.

34. Dundas J, et al. (2006) CASTp: computed atlas of surface topography of proteins with structural and topographical mapping of functionally annotated residues. *Nucleic Acids Res* 34(Web Server issue):W116-118.

35. Hernandez M, Ghersi D, Sanchez R (2009) SITEHOUND-web: a server for ligand binding site identification in protein structures. *Nucleic Acids Res* 37(suppl 2):W413–W416.

36. Consortium TU (2015) UniProt: a hub for protein information. *Nucleic Acids Res* 43(D1):D204–D212.

37. Boeckmann B, et al. (2005) Protein variety and functional diversity: Swiss-Prot annotation in its biological context. *C R Biol* 328(10–11):882–899.

38. Pettersen EF, et al. (2004) UCSF Chimera--a visualization system for exploratory research and analysis. *J Comput Chem* 25(13):1605–1612.

39. Irwin JJ, Sterling T, Mysinger MM, Bolstad ES, Coleman RG (2012) ZINC: A Free Tool to Discover Chemistry for Biology. *J Chem Inf Model* 52(7):1757–1768.

40. Brooks BR, et al. (2009) CHARMM: the biomolecular simulation program. *J Comput Chem* 30(10):1545–1614.

41. Haberthür U, Caflisch A (2008) FACTS: Fast analytical continuum treatment of solvation. *J Comput Chem* 29(5):701–715.